Ruxolitinib Impairs Chemokine-Directed Migration and Delays Activation of Human Cytotoxic T Lymphocytes by Modulating P-Glycoprotein Function

Kipchumba Biwott , Algirmaa Lkhamkhuu , Nimrah Ghaffar , Albert Bálint Papp , Nastaran Tarban , Katalin Goda , Zsolt Bacso *

Posted Date: 8 May 2025

doi: 10.20944/preprints202505.0512.v1

Keywords: Ruxolitinib; Cytotoxic T lymphocytes (CTLs); P-glycoprotein (Pgp, MDR1, ABCB1); T cell activation; Chemokine-driven migration; JAK-STAT signaling; Immune modulation

 doi:10.20944/preprints202505.0512.v1

Article

Ruxolitinib Impairs Chemokine-Directed Migration and Delays Activation of Human Cytotoxic T Lymphocytes by Modulating P-Glycoprotein Function

Kipchumba Biwott [1,2,3], Algirmaa Lkhamkhuu [1,2,4], Nimrah Ghaffar [1,2], Albert Bálint Papp [5,6], Nastaran Tarban [2,5], Katalin Goda [1,2] and Zsolt Bacso [1,2,7,*]

[1] Department of Biophysics and Cell Biology, Faculty of Medicine, University of Debrecen, Debrecen 4032, Hungary
[2] Doctoral School of Molecular Cell and Immune Biology, University of Debrecen, Faculty of Medicine, Debrecen 4032, Hungary
[3] Department of Biological and Life Sciences, Technical University of Kenya, Kenya
[4] Department of Biomedicine and Pharmacy, Darkhan-Uul Medical School, Mongolian National University of Medical Sciences, Mongolia
[5] Department of Biochemistry and Molecular Biology, Faculty of Medicine, University of Debrecen, Debrecen 4032, Hungary
[6] Doctoral School of Dental Sciences, Faculty of Medicine, University of Debrecen, Debrecen 4032, Hungary
[7] Dean's office, Faculty of Pharmacy, University of Debrecen, Debrecen 4032, Hungary
* Correspondence: bacso@med.unideb.hu

Abstract: Cytotoxic T lymphocytes (CTLs) rely on tightly regulated activation, efflux capacity, and migration to maintain immune surveillance and establish memory pools. Modulation of these pathways can profoundly affect T cell differentiation and function. We investigated how ruxolitinib, a clinically approved JAK1/2 inhibitor, impacts P-glycoprotein (Pgp, MDR1, ABCB1) expression and function, T cell activation markers, and chemokine-driven transmigration in human $CD8^+$ T cells. Ruxolitinib modulated Pgp activity at multiple levels. It induced and stabilized ABCB1 mRNA during acute TCR activation, directly inhibited Pgp efflux function, and stimulated basal ATPase activity in a manner similar to the known Pgp substrate verapamil. Functional assays confirmed ruxolitinib as a Pgp modulator and inducer. In addition, treatment with ruxolitinib suppressed TCR-induced upregulation of PD-1 and CD8 surface markers, suggesting interference with activation-associated differentiation pathways. Finally, ruxolitinib significantly impaired CCL19-driven transmigration of CTLs across human umbilical vein endothelial cell (HUVEC) monolayers at clinically relevant concentrations, highlighting its effect on lymphoid homing mechanisms. Our findings reveal that ruxolitinib profoundly reshapes CTL function by altering efflux regulation, activation dynamics, and migratory behavior. These insights have important implications for optimizing JAK-targeted therapies in immune modulation, vaccination, transplantation, and memory T cell-based immunotherapies.

Keywords: ruxolitinib; cytotoxic T lymphocytes (CTLs); P-glycoprotein (Pgp; MDR1; ABCB1); T cell activation; chemokine-driven migration; JAK-STAT signaling; immune modulation

1. Introduction

P-glycoprotein (Pgp, also known as MDR1 and encoded by the ABCB1 gene) is a critical member of the ATP-binding cassette (ABC) family of membrane transporters. It functions as an efflux pump, transporting a wide range of xenobiotics, toxins, and cytostatic drugs out of cells [1–3]. Pgp is widely expressed in protective barriers such as the blood-brain barrier, gastrointestinal tract, liver, kidneys,

 doi:10.20944/preprints202505.0512.v1

and placental tissues. Notably, Pgp is expressed in immune cells, including natural killer (NK) cells, dendritic cells (DCs), antigen-presenting cells, and both $CD4^+$ and $CD8^+$ T lymphocytes [4–7].

In $CD8^+$ T cells, Pgp plays key roles in mediating multidrug resistance, regulating immune responses, protecting against reactive oxygen species generated during early T-cell receptor (TCR) activation, and facilitating T-cell activation and expansion [5,8,9]. Beyond its role in drug efflux, Pgp also contributes to the release of pro-inflammatory cytokines and cholesterol, with broad implications for immune function and drug bioavailability [10].

The impact of Pgp-mediated drug resistance is well documented in oncology, particularly regarding tyrosine kinase inhibitors (TKIs) such as imatinib in chronic myeloid leukemia (CML) [11]. In myeloproliferative neoplasms (MPNs), disorders frequently associated with JAK-STAT pathway mutations, Pgp similarly contributes to drug resistance [12]. While JAK1 and JAK2 proteins are essential for cytokine-mediated signaling in normal hematopoietic cells, their dysregulation promotes oncogenesis in conditions such as polycythemia vera, essential thrombocythemia, primary myelofibrosis, and acute lymphoblastic leukemia [13]. These insights led to the development of JAK inhibitors, notably ruxolitinib, a clinically approved non-selective JAK1/2 inhibitor for the treatment of myelofibrosis and other MPNs [14–16]. Ruxolitinib is also increasingly used for immunomodulation in conditions like graft-versus-host disease (GVHD) [15,17].

Ruxolitinib's pharmacokinetics are primarily influenced by cytochrome P450 enzymes CYP3A4 and CYP2C9, with known interactions that affect its metabolism and efficacy [18]. In addition to CYP-mediated metabolism, ruxolitinib's interaction with Pgp could significantly impact its distribution, bioavailability, and therapeutic activity, particularly in patients receiving combination therapies involving other Pgp substrates. Indeed, genetic inactivation of Pgp has been shown to enhance ruxolitinib's inhibition of T cell proliferation, suggesting that Pgp-mediated efflux may attenuate its immunosuppressive effects [17].

Programmed cell death-1 (PD-1, CD279), a member of the CD28 family, is an inhibitory receptor expressed at low levels on resting T and B cells. Upon TCR or BCR activation, PD-1 is upregulated to regulate immune tolerance and prevent autoimmunity [19,20]. Various cancers exploit PD-1 signaling to evade immune detection, and ruxolitinib has been shown to modulate PD-1 pathways, enhancing anti-tumor immune responses [21]. However, while Pgp's role as an efflux transporter is well established, its interaction with ruxolitinib remains poorly understood. It is unclear whether Pgp acts as a substrate, modulator, inhibitor, or inducer.

In this study, we investigated the dynamic regulation of Pgp and CD8 expression in human cytotoxic T lymphocytes under resting and antigen-primed conditions. We assessed the functional interaction between ruxolitinib and Pgp using specific and non-specific Pgp inhibitors, fluorescent substrate assays, and ATPase activity measurements. Our results demonstrate that while ruxolitinib inhibits Pgp efflux function, this occurs at concentrations higher than typical therapeutic plasma levels. However, ruxolitinib directly interacts with Pgp, as evidenced by its stimulation of Pgp ATPase activity. Furthermore, its interference with verapamil-induced transporter activation suggests potential drug-drug interactions. Additionally, ruxolitinib delays the downregulation of ABCB1 mRNA during T-cell activation, suppresses PD-1 upregulation, and significantly impairs CCL19-directed CTL transmigration across human endothelial barriers. These findings suggest that ruxolitinib modulates T cell differentiation, trafficking, and efflux capacity, with important implications for immune modulation and therapeutic strategies.

2. Results

To systematically investigate the influence of ruxolitinib on cytotoxic T lymphocyte (CTL) phenotype and function, we carried out a series of molecular, biochemical, and cellular assays. First, we characterized baseline and antigen-induced changes in P-glycoprotein and CD8 expression, then evaluated ruxolitinib’s effects on Pgp mRNA levels, transporter activity, activation marker expression, and chemotactic behavior.

 doi:10.20944/preprints202505.0512.v1

2.1. Dynamic Expression of P-Glycoprotein and CD8 in Quiescent and Antigen-Primed Human Lymphocytes.

Pgp plays a critical role in mediating drug efflux and regulating immune cell function. Its expression is dynamically modulated during T cell activation and differentiation. To investigate changes in Pgp expression, human peripheral blood lymphocytes were co-cultured with proliferation-inhibited JY cells in a mixed lymphocyte culture assay. The JY cell line, derived from human B-lymphoblasts, constitutively expresses high levels of the MHC class I molecule A*02:01 on its surface. This makes it highly suitable as an antigen-presenting cell for stimulating T cell responses [22,23].

P-glycoprotein expression was evaluated in quiescent peripheral blood $CD8^+$ lymphocytes (CTL13, CTL14) and compared with $CD8^+$ lymphocytes primed with JY cells (CTL1, CTL4), with each blood sample derived from a different human donor (Figure 1). The priming procedure involved culturing peripheral blood lymphocytes with JY cells biweekly over a period of one month, thereby facilitating the differentiation of mature cytotoxic T lymphocytes and memory T cells. Unprimed lymphocytes (CTL13, CTL14) exhibited slightly but significantly higher levels of Pgp expression compared to the JY-primed lymphocytes (CTL1, CTL4) (Figure 1A). This modest decrease in average Pgp expression observed after repeated antigenic stimulation likely reflects the pronounced transition of T cells from a naïve to an effector phenotype, accompanied by the generation of memory cells, each population demonstrating distinct patterns of Pgp expression.

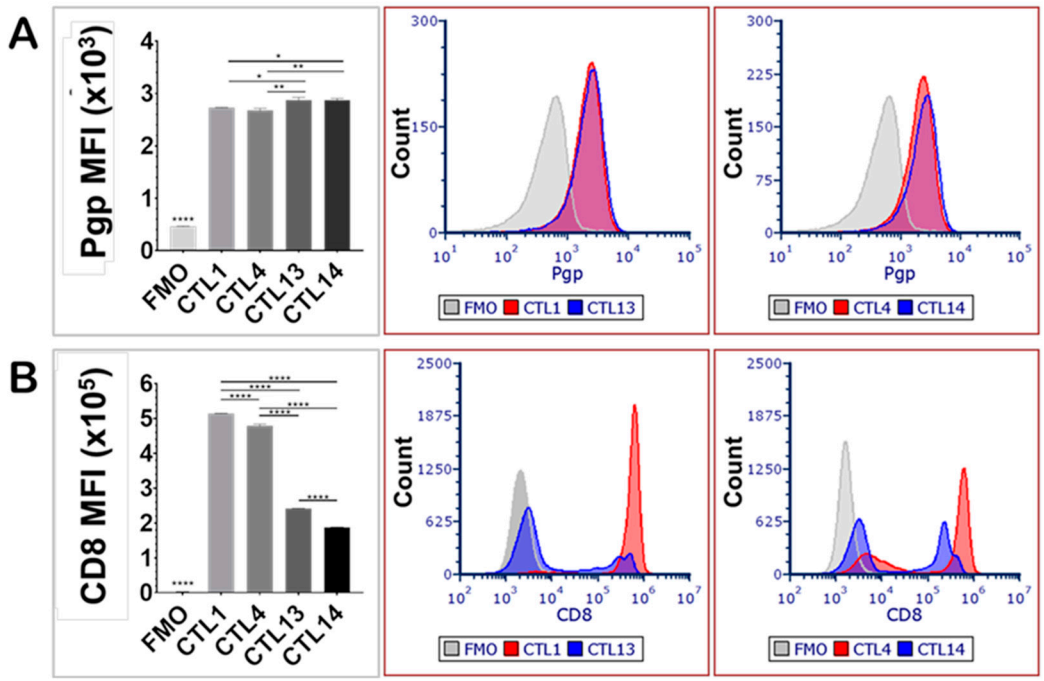

Figure 1. Expression of P-glycoprotein and CD8 on JY-primed and unprimed human $CD8^+$ T lymphocytes. Pgp expression decreased, while CD8 expression increased upon activation. (A) Mean fluorescence intensity (MFI) and fluorescence intensity distribution overlays of Pgp in JY-primed (CTL1, CTL4) and unprimed (CTL13, CTL14) cytotoxic T lymphocyte (CTL) samples from different human donors. (B) MFI and fluorescence distribution overlays of CD8 expression in CTL1, CTL4, CTL13, and CTL14 donor samples. Statistical comparisons between groups were performed using one-way ANOVA followed by Tukey's multiple comparison test (n=3). Significance levels are indicated as *$p < 0.05$, **$p < 0.01$, ***$p < 0.001$. Error bars represent mean ± SEM.

In contrast, CD8 expression was significantly elevated in JY-primed CTLs (CTL1, CTL4) compared to their unprimed counterparts (CTL13, CTL14) (Figure 1B). This increase in CD8 expression likely reflects enhanced T cell activation, differentiation, and cytotoxic potential resulting from repeated antigen stimulation, thereby promoting robust $CD8^+$ cellular immune responses in the mixed lymphocyte cultures. Notably, CD8 expression levels showed considerable variation among

 doi:10.20944/preprints202505.0512.v1

individual donors, underscoring donor-dependent heterogeneity in protein expression. In contrast, inter-donor variability in Pgp expression was not statistically significant.

2.2. Ruxolitinib Modulates P-Glycoprotein mRNA Expression in TCR-Activated Human T Cells

ABCB1, the gene encoding P-glycoprotein, plays a pivotal role in chemoresistance and immune cell function by mediating the efflux of a wide range of xenobiotics. To investigate the potential interaction between the Janus kinase (JAK) inhibitor ruxolitinib and Pgp, we assessed its effects on ABCB1 mRNA expression in primary human T lymphocytes.

We first assessed ABCB1 mRNA expression in JY-primed lymphocyte cultures, which are predominantly composed of $CD8^+$ cytotoxic T lymphocytes, and compared these levels to a positive control cell line known to highly express human Pgp. The NIH-3T3 MDR1 cell line, mouse fibroblasts transfected with the human ABCB1 gene, served as the positive control, while untransfected NIH-3T3 parental cells served as the negative control (Figure 2A). When normalized to CTL expression levels, NIH-3T3 MDR1 cells expressed approximately 500-fold higher levels of ABCB1 mRNA, whereas expression in the untransfected NIH-3T3 cells was undetectable. Gene expression normalization was performed using both human and mouse ACTB (β-actin) and GAPDH reference genes. For consistency, all figures display normalization to ACTB, which yielded lower inter-treatment variability in human lymphocytes compared to GAPDH.

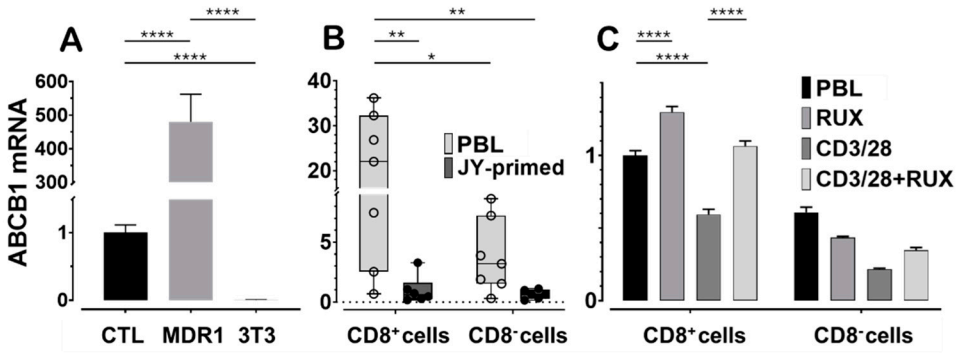

Figure 2. Human P-glycoprotein transporter (ABCB1) mRNA is expressed in cytotoxic T lymphocytes. Gene expression levels were normalized to ACTB (β-actin). (A) ABCB1 mRNA expression in JY-primed cultured human cytotoxic T lymphocytes compared to control cell lines: ABCB1-transfected (MDR1, expressing human ABCB1) and untransfected NIH-3T3 mouse fibroblasts. Values are presented as fold changes relative to the average mRNA expression in CTLs. (B) ABCB1 mRNA levels in flow cytometry-sorted $CD8^+$ and $CD8^-$ T cells from freshly isolated peripheral blood lymphocytes (PBLs) and JY-primed CTLs cultured for one month from the same donors. Values are expressed as fold changes relative to the average expression in JY-primed $CD8^+$ CTLs. (C) ABCB1 mRNA expression in flow cytometry-sorted $CD8^+$ and $CD8^-$ T cells from freshly isolated PBLs were activated or not for 72 hours with anti-CD3/CD28 beads, either in the presence or absence of 100 nM ruxolitinib (RUX), a JAK1/2 kinase inhibitor. Values are shown as fold changes relative to the average expression in unstimulated PBLs. Statistical comparisons were performed using one- or two-way ANOVA, followed by Dunnett's or Tukey's multiple comparisons tests, as appropriate. Significance levels are indicated by asterisks (*$p < 0.05$; **$p < 0.01$; ****$p < 0.0001$). Error bars represent the mean ± SEM (n = 3) in panels A and C. In panel B, the median, interquartile range (second and third quartiles), and 95% confidence intervals are shown (n = 6–7).

Next, we examined baseline variability in ABCB1 mRNA levels between $CD8^+$ T cells isolated from peripheral blood lymphocytes and those from JY-primed CTL cultures generated from five independent human donors (Figure 2B). JY cells provided alloantigenic stimulation, mimicking physiological T cell priming. After this priming, ABCB1 mRNA levels were reduced by approximately 95%, or to one-twentieth of those observed in naive PBL-derived $CD8^+$ cells. Although substantial donor-to-donor variation was observed in the naïve cell populations, a consistent

 doi:10.20944/preprints202505.0512.v1

decrease in ABCB1 expression was noted across nearly all donors after long-term activation. This trend parallels our earlier findings at the protein level and is consistent with T cell maturation, in which cells shift from naive and memory states toward more differentiated effector phenotypes [23]

Finally, we investigated the immediate impact of ruxolitinib on ABCB1 expression in $CD8^+$ T lymphocytes undergoing acute T cell receptor (TCR) stimulation (Figure 2C). PBLs were stimulated for 72 hours using anti-CD3/CD28 beads, which led to a reduction in ABCB1 mRNA expression, consistent with the trend observed in the one-month JY-priming model. Notably, co-treatment with 100 nM ruxolitinib attenuated this decrease and appeared to sustain ABCB1 expression in both $CD8^+$ and $CD8^-$ lymphocyte populations. These findings suggest that ruxolitinib, a JAK1/2 inhibitor, may modulate Pgp expression by interfering with TCR signaling pathways involved in T cell activation and differentiation. Furthermore, this effect occurs not only at the protein level but is also evident at the mRNA level. The observed trends were consistent across both short-term activated naive T cells and long-term cultured JY-primed effector/memory CTLs [23].

2.3. Dose-Dependent Inhibition of P-Glycoprotein Activity by Ruxolitinib and Zosuquidar in Cytotoxic T Lymphocytes

To evaluate the presence of functional P-glycoprotein in human cytotoxic T lymphocytes, we monitored its transporter activity using a calcein efflux assay [24–26]. Calcein-AM is a fluorescent, nonpolar substrate of Pgp that becomes fluorescent upon intracellular esterase cleavage. Its intracellular accumulation is inversely proportional to Pgp efflux activity. To quantify transporter function, we calculated the transport activity factor (TAF), representing the fractional increase in calcein accumulation in the presence versus absence of a Pgp inhibitor.

To validate Pgp activity and evaluate its pharmacological inhibition, we generated dose-response curves using the third-generation Pgp-specific inhibitor zosuquidar. These curves were established in both NIH-3T3 cells overexpressing human MDR1 (NIH-3T3 MDR1) and in primary human CTLs. In both systems, zosuquidar effectively inhibited Pgp-mediated efflux in a dose-dependent manner (Figure 3). NIH-3T3 MDR1 cells exhibited a high sensitivity to zosuquidar, with an IC_{50} range of 1.779×10^{-7} to 2.847×10^{-7} M. In contrast, CTLs displayed a right-shifted inhibition curve, with an IC_{50} range of 1.809×10^{-6} to 3.498×10^{-6} M, consistent with their lower baseline Pgp expression in these cells.

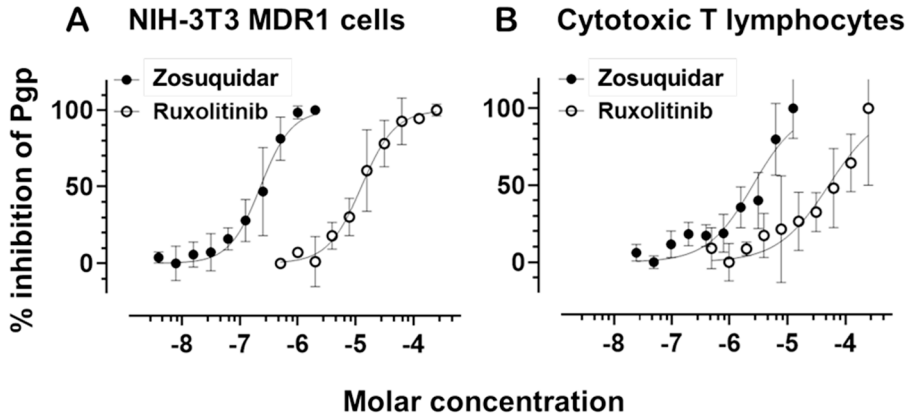

Figure 3. Dose-dependent inhibition of P-glycoprotein activity by ruxolitinib and zosuquidar. (A) NIH-3T3 cells stably expressing human MDR1 and (B) primary human cytotoxic T lymphocytes were analyzed using a calcein-AM efflux assay to assess Pgp activity. Cells were treated with increasing concentrations of either zosuquidar (filled circles) or ruxolitinib (open circles), and intracellular fluorescence was measured to determine the percentage inhibition of Pgp. Data represent mean ± SD from triplicate measurements. Zosuquidar showed potent inhibition in both cell types, with lower IC_{50} values in NIH-3T3 MDR1 cells compared to CTLs. Ruxolitinib inhibited Pgp with significantly higher IC_{50} values, indicating lower potency in both cell types.

 doi:10.20944/preprints202505.0512.v1

To optimize assay sensitivity in CTLs, we reduced the concentration of calcein-AM to account for their lower transporter expression relative to NIH-3T3 MDR1 cells. This adjustment enabled a clear and quantifiable dose-dependent inhibition of Pgp, confirming that zosuquidar remains effective in primary CTLs, albeit at higher concentrations than in MDR1-overexpressing cell lines.

Next, we evaluated the JAK1/2 inhibitor ruxolitinib for its potential to modulate Pgp function. Ruxolitinib also produced a measurable, dose-dependent inhibition of calcein efflux in both NIH-3T3 MDR1 cells and CTLs. In NIH-3T3 MDR1 cells, the IC_{50} for ruxolitinib ranged from 1.002×10^{-5} to 1.572×10^{-5} M, indicating moderate inhibitory potency. In CTLs, the IC_{50} was higher, between 3.003×10^{-5} and 8.543×10^{-5} M, suggesting reduced affinity or indirect modulation of Pgp activity. The dose-response curves for ruxolitinib were substantially right-shifted in both systems compared to zosuquidar, suggesting a weaker interaction with the transporter. Nevertheless, the inhibition profile in CTLs indicates that ruxolitinib may act as a low-affinity Pgp substrate or modulator.

2.4. Ruxolitinib Directly Stimulates P-Glycoprotein ATPase Activity and Interferes with Verapamil-Induced Activation

To evaluate the direct interaction of ruxolitinib with Pgp, we performed ATPase activity assays using membrane preparations from NIH-3T3 MDR1 cells. Although our fluorescent substrate accumulation assay suggested functional inhibition of Pgp, the ATPase assay provides a more direct readout of transporter interaction. Changes in ATP hydrolysis reflect alterations in the conformational cycling triggered by substrate or inhibitor binding.

We first assessed basal ATPase activity and examined whether ruxolitinib, zosuquidar (ZQ), or cyclosporine A (CSA) could modulate it. As shown in Figure 4, ruxolitinib stimulated basal Pgp ATPase activity in a concentration-dependent manner with doses tested at 1 μM, 10 μM, and 100 μM. The highest dose (100 μM) more than doubled basal ATPase activity compared to control conditions, with the increase being statistically significant ($p < 0.01$). The effect of 100 μM ruxolitinib was comparable to that of verapamil (40 μM), a well-characterized Pgp activator, which also significantly elevated ATPase activity ($p < 0.001$).

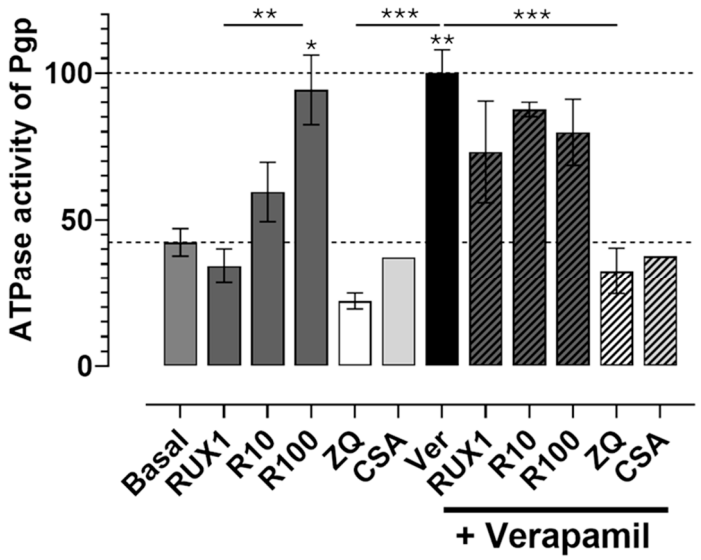

Figure 4. Ruxolitinib activates the ATPase activity of P-glycoprotein and interferes with other activators. Ruxolitinib (RUX) increased basal ATPase activity in a dose-dependent manner at concentrations of 1 μM (RUX1), 10 μM (R10), and 100 μM (R100), with R100 significantly enhancing basal ATPase activity to levels comparable to those induced by verapamil (Ver). Zosuquidar (ZQ) and cyclosporin A (CSA) reduced both basal and verapamil-stimulated ATPase activity. Co-treatment with ruxolitinib and verapamil showed additive or competitive effects depending on ruxolitinib concentration. Data represent mean ± SEM; significance determined

 doi:10.20944/preprints202505.0512.v1

by one-way ANOVA followed by post-hoc multiple comparisons: *p < 0.05;**p < 0.01; ***p < 0.001(n = 3, except CSA n = 1).

In contrast, both ZQ (10 μM) and CSA (20 μM), known Pgp inhibitors, significantly reduced basal ATPase activity compared to control ($p < 0.01$ for ZQ), confirming their inhibitory role on transporter function.

Next, we investigated how ruxolitinib modulates verapamil-induced ATPase stimulation. Co-treatment with verapamil and increasing concentrations of ruxolitinib revealed concentration-dependent interference: at lower ruxolitinib concentrations (1–10 μM), ATPase activation appeared additive to verapamil's effect. However, at 100 μM ruxolitinib, ATPase activity was significantly reduced compared to verapamil alone ($p < 0.001$), suggesting a competitive or inhibitory interaction at higher drug levels.

Similarly, ZQ and CSA were effective in completely suppressing verapamil-induced ATPase stimulation ($p < 0.001$ compared to verapamil alone), consistent with their potent inhibitory action.

Together, these results demonstrate that ruxolitinib directly stimulates basal Pgp ATPase activity in a concentration-dependent and statistically significant manner and can interfere with ATPase activation by other substrates, such as verapamil. This behavior strongly supports the interpretation that ruxolitinib acts as a direct Pgp-interacting compound, likely behaving as a transported substrate or modulator, with potential implications for drug-drug interactions involving Pgp.

2.5. Ruxolitinib Impedes PD-1 Expression and Modulates CD8 and Pgp Levels in Human CD8⁺ T Cells Following Acute Activation

Ruxolitinib is known to delay lymphocyte maturation, a property leveraged clinically in graft-versus-host disease and myeloproliferative disorders where altered JAK-STAT signaling drives aberrant T cell proliferation. To determine whether ruxolitinib's maturation-delaying effect could be recapitulated in vitro, we activated human peripheral blood lymphocytes with CD3/CD28 beads for 72 hours. Then, we assessed surface expression of PD-1, CD8, and P-glycoprotein.

Given our focus on $CD8^+$ cytotoxic T lymphocytes, we analyzed the $CD8^+$ and $CD8^-$ subsets separately by flow cytometry. Cells were stained with fluorophore-conjugated antibodies against CD8, PD-1, and Pgp, and mean fluorescence intensity (MFI) was quantified.

As shown in Figure 5, acute CD3/CD28 activation robustly upregulated PD-1 expression in $CD8^+$ cells ($p < 0.0001$), confirming successful T cell activation. Ruxolitinib treatment significantly blunted this induction, resulting in markedly lower PD-1 levels than activated, untreated controls ($p < 0.0001$), suggesting that ruxolitinib delays or attenuates activation-associated phenotypic maturation.

Similarly, CD8 expression levels were significantly increased upon CD3/CD28 stimulation ($p < 0.0001$). However, this upregulation was partially inhibited by ruxolitinib ($p < 0.0001$), further supporting an inhibitory effect on activation-induced changes. For Pgp, CD3/CD28 activation also significantly upregulated surface expression ($p < 0.0001$), but ruxolitinib treatment significantly suppressed this induction, although to a lesser extent than for PD-1.

In contrast, the $CD8^-$ population exhibited minimal changes in PD-1, CD8, or Pgp expression across conditions, and the differences were not statistically significant. This suggests that ruxolitinib's effects are more pronounced in $CD8^+$ T cells.

Overall, these findings demonstrate that ruxolitinib impedes PD-1 induction and modulates CD8 and Pgp expression in activated $CD8^+$ T lymphocytes, reinforcing its role as an inhibitor of activation-associated maturation events in T cells.

 doi:10.20944/preprints202505.0512.v1

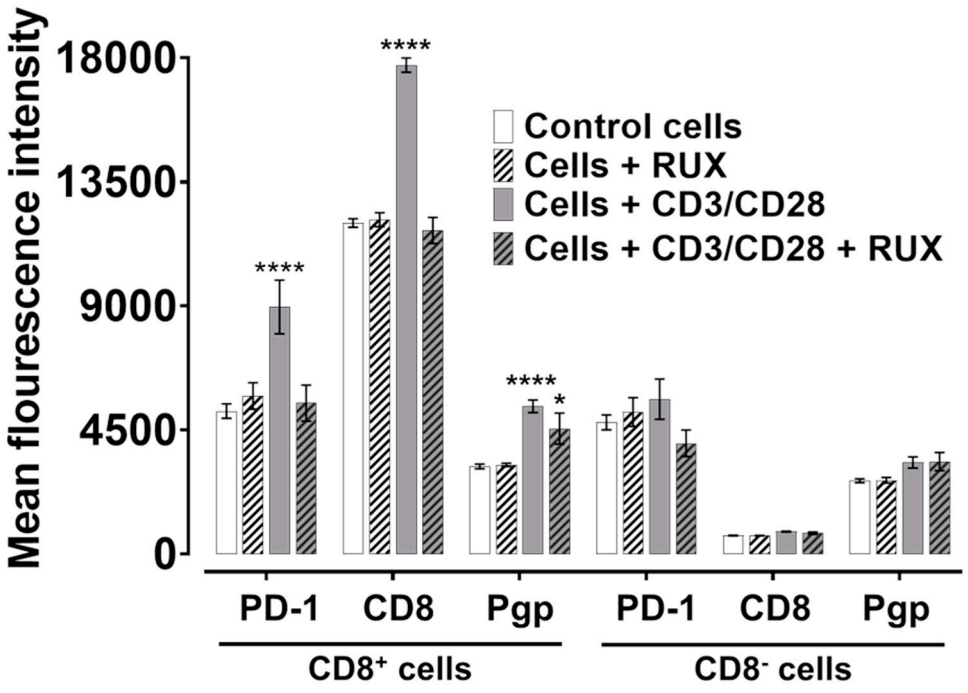

Figure 5. Ruxolitinib modulates P-glycoprotein and CD8 surface levels on sorted human cytotoxic T lymphocytes and inhibits PD-1 expression during acute CD3/CD28-mediated activation. Peripheral blood mononuclear cells were activated with CD3/CD28 beads for 72 hours and treated either with ruxolitinib (100 nM) or left untreated. Following incubation, cells were stained with fluorophore-conjugated anti-Pgp, anti-PD-1, and anti-CD8 antibodies and analyzed by flow cytometry. Fluorescence intensity was quantified in 20,000 cells per condition. Data represent mean ± SEM from three independent experiments (n = 3). Group comparisons were analyzed by one-way ANOVA followed by Tukey's multiple comparison test (*$p < 0.05$; ****$p < 0.0001$).

2.6. Ruxolitinib Inhibits CCL19-Induced Transmigration of Human Cytotoxic T Lymphocytes Across Endothelial Barriers

One of the key functional properties of memory T cells is their regulated migratory capacity, which is essential for long-term survival by enabling trafficking to supportive niches such as lymph nodes and bone marrow. To assess whether ruxolitinib influences lymph node-directed migration, we evaluated the ability of human cytotoxic T lymphocytes to transmigrate across monolayers of human umbilical vein endothelial cells (HUVECs) in response to the chemokine CCL19.

At a pharmacologically relevant concentration (100 nM), ruxolitinib significantly inhibited CCL19-induced CTL transmigration compared to untreated controls ($p < 0.05$; Figure 6A). Notably, while suppression of Pgp efflux required higher concentrations, inhibition of CTL transmigration occurred within the therapeutic range. These findings suggest that ruxolitinib impairs the ability of CTLs to migrate across endothelial barriers in response to lymphoid chemokine signals.

Next, we examined the dose-dependence of this effect. As shown in Figure 6B, increasing concentrations of ruxolitinib progressively reduced CTL migration toward CCL19 (500 ng/mL), with significant inhibition observed at concentrations as low as 0.4 μM ($p < 0.05$), becoming more pronounced at higher concentrations. In contrast, spontaneous transmigration without CCL19 (negative control) remained minimal across all conditions.

Finally, we confirmed that CCL19 induced a robust, dose-dependent enhancement of CTL transmigration across HUVECs, as shown in Figure 6C, with maximal responses seen at the highest tested concentration (500 ng/mL, $p < 0.01$ compared to lower concentrations).

Collectively, these results demonstrate that ruxolitinib significantly impairs CTL chemotaxis across endothelial barriers in a concentration-dependent manner. This highlights a potential modulatory effect of JAK inhibition on T cell trafficking in immune environments.

 doi:10.20944/preprints202505.0512.v1

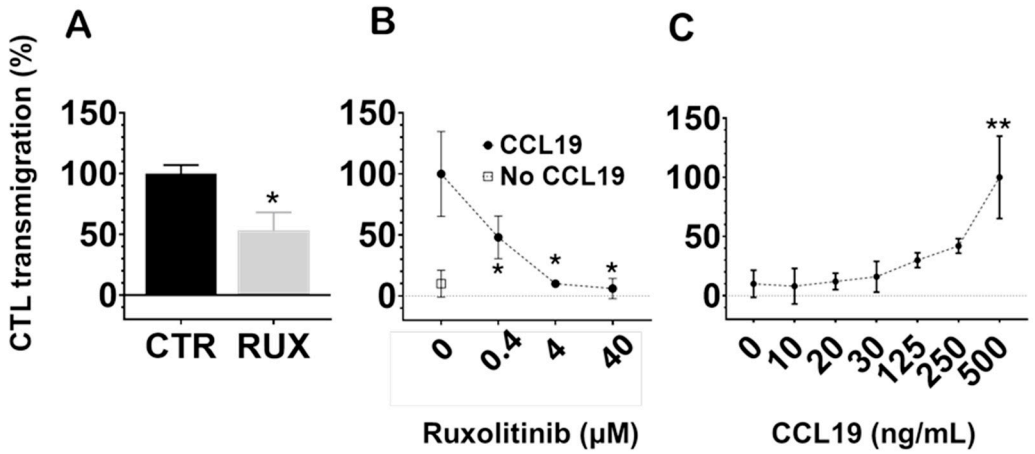

Figure 6. Ruxolitinib inhibits CTL transmigration induced by CCL19 through HUVEC monolayers. (A) Ruxolitinib (100 nM) significantly reduced CCL19-driven CTL transmigration compared to untreated control cells (CTR) (*$p < 0.05$). (B) Ruxolitinib inhibited CCL19-induced CTL chemotaxis in a concentration-dependent manner, with significant effects observed at 0.4 μM and above (*$p < 0.05$ compared to untreated CCL19-stimulated cells). (C) CCL19 induced a dose-dependent increase in CTL transmigration across HUVECs, with maximal migration observed at 500 ng/mL ($p < 0.01$ compared to lower concentrations). Data represent mean ± SEM from at least three independent experiments ($n \geq 3$). Statistical analysis was performed using one-way ANOVA followed by Tukey's multiple comparison test.

3. Discussion

Our study provides new mechanistic insights into how ruxolitinib modulates cytotoxic T lymphocyte function through both direct and indirect effects on P-glycoprotein expression and activity, T cell activation marker expression, and chemokine-driven migration. We show that ruxolitinib not only alters Pgp transporter function at the transcriptional and protein activity levels but also impairs PD-1 upregulation and CD8 surface expression during TCR stimulation. Moreover, ruxolitinib significantly inhibits CCL19-mediated CTL transmigration across endothelial barriers, suggesting that JAK inhibition may broadly affect T cell trafficking toward lymphoid niches. These findings highlight the multifaceted impact of ruxolitinib on key processes essential for memory T cell development, immune surveillance, and potential therapeutic targeting.

3.1. Ruxolitinib Modulates P-Glycoprotein Expression and Activity

We hypothesized that P-glycoprotein plays a functional role in the persistence of long-lived, stem-like T lymphocytes and that their Pgp expression is dynamically regulated during T cell differentiation [23]. We observed a slight but significant decrease in Pgp protein expression in JY-primed cytotoxic T lymphocytes compared to unprimed cells. In parallel, ABCB1 mRNA expression was approximately 20-fold higher in naive $CD8^+$ T cells than in long-term activated effector cells, supporting the notion that T cell maturation is associated with Pgp downregulation.

Excited by previous reports linking ABCB1 expression to ruxolitinib efficacy in vitro and in vivo [17], we sought to characterize the direct interaction between ruxolitinib and Pgp. Using a calcein-AM efflux assay [24–26], we measured inhibitory concentrations for ruxolitinib in both NIH-3T3 MDR1-overexpressing cells and primary $CD8^+$ lymphocytes. We found that ruxolitinib inhibited Pgp function with an IC_{50} of approximately 13 μM in NIH-3T3 MDR1 cells and approximately 58 μM in $CD8^+$ T cells. These concentrations are higher than typical therapeutic plasma levels, suggesting that significant Pgp inhibition by ruxolitinib may require local accumulation, which is supported by clinical observations where Pgp expression dampens ruxolitinib efficacy [17]. However, the IC_{50} for fluorescent marker retention does not precisely reflect the biological activity of ruxolitinib, but rather

 doi:10.20944/preprints202505.0512.v1

indicates its interaction with P-glycoprotein. ATPase assays further endorsed this direct interaction of ruxolitinib with Pgp [27–31], which showed that ruxolitinib, like verapamil, significantly activated Pgp ATPase activity in a concentration-dependent manner, achieving maximal stimulation at 100 μM.

Importantly, ruxolitinib not only stimulated basal ATPase activity but also interfered with verapamil-induced activation, further corroborating its direct interaction with the transporter and suggesting a competitive or modulatory effect. Based on Seelig's categorization of Pgp-interacting drugs [10], ruxolitinib, a drug with a lower molecular weight than the critical threshold of 450, can be classified as a modulator. It acts as a substrate for Pgp, stimulates ATPase activity, and potentially competes with other substrates. Furthermore, it induces the Pgp mRNA expression. Unlike classic inhibitors as cyclosporin A or zosuquidar, ruxolitinib did not suppress ATPase basal activity, but rather enhanced it. This reflects a complex modulatory interaction that may impact drug-drug interactions and ruxolitinib's own bioavailability in T cell subsets expressing Pgp.

3.2. Effects on T Cell Activation and Phenotypic Maturation

Beyond its effects on Pgp, ruxolitinib modulated key markers of T cell activation. During acute TCR stimulation with CD3/CD28 beads, we observed a robust upregulation of PD-1 expression, which was significantly inhibited by ruxolitinib treatment. CD8 expression and Pgp surface levels were also affected. Ruxolitinib fully or partially attenuated the upregulation of these markers following activation, respectively. Our findings align with previous reports showing that repeated TCR activation increases PD-1 expression, whereas ruxolitinib treatment suppresses PD-1 signaling [32,33].

Interestingly, while changes in Pgp protein expression after activation were modest (a ~50% increase after 72 hours of CD3/CD28 stimulation, and a slight decrease after 30 days of JY priming), mRNA changes were far more pronounced: ABCB1 mRNA levels decreased by approximately 20-fold following short-term activation and by about ~50% after prolonged activation. These discrepancies between protein and mRNA dynamics likely reflect the heterogeneity of T cell subpopulations. Naive, effector, and memory cells differentially express Pgp, highlighting the complexity of interpreting average expression levels across diverse cellular subsets [23].

Together, these findings support the idea that ruxolitinib delays T cell differentiation by interfering with activation-associated signaling pathways, thereby maintaining a more naive or less differentiated phenotype.

3.3. Impairment of Chemokine-Directed T Cell Migration

One of the hallmarks of functional lymphocytes, particularly memory T cells, is their capacity for directed migration toward tissue niches such as lymph nodes and bone marrow [34]. Using a transmigration assay across human endothelial cell layers, we found that ruxolitinib significantly inhibited CCL19-induced chemotaxis of CTLs in a concentration-dependent manner.

This is a novel finding in human $CD8^+$ T cells. Previous mouse studies suggested that ruxolitinib can impair dendritic cell and lymphocyte transmigration, possibly through both JAK1/2 inhibition and off-target effects on ROCK kinases [35,36]. In human systems, ruxolitinib has been reported to inhibit CXCL9, CXCL10, and CXCL11/CXCR3-axis-directed migration in $CD4^+$ T lymphocytes, and to reduce lymph node-directed migration of human dendritic cells, along with other immunomodulatory effects [33,37,38]. This study is the first to demonstrate that ruxolitinib impairs CCL19-driven migration of human $CD8^+$ cytotoxic T cells.

Notably, although inhibition of Pgp efflux function and modulation of ATPase activity by ruxolitinib required concentrations higher than typical therapeutic levels, impairment of CCL19-driven CTL transmigration was observed at clinically relevant serum concentrations, suggesting distinct concentration thresholds for its effects on efflux activity versus migratory behavior.

These results suggest that JAK1/2 signaling is critical not only for cytokine responsiveness but also for chemokine-driven locomotion in human lymphocytes.

 doi:10.20944/preprints202505.0512.v1

Moreover, the additive inhibitory effect of ruxolitinib on human dendritic cells and $CD8^+$ T cells may underlie its therapeutic efficacy in conditions such as graft-versus-host disease (GVHD) and myeloproliferative disorders, and may open new avenues for therapeutic applications targeting immune cell trafficking.

3.4. Clinical and Therapeutic Implications

The ability of ruxolitinib to modulate Pgp expression and function, suppress T cell activation markers, and inhibit chemokine-directed migration has significant therapeutic implications. These findings, together with others and our earlier observations [23] suggest that ruxolitinib can alter T cell differentiation pathways, may impair trafficking to inflammatory niches, and possibly influence immune exhaustion programs by reducing PD-1 expression. This multilayered modulation could enhance its utility in preventing aberrant T cell activation in autoimmune diseases, promoting tolerance in transplantation settings, and potentially reshaping immune memory in cancer immunotherapy. Although ruxolitinib promotes T cell memory differentiation, its inhibitory effect on bone marrow-directed migration suggests that, when combined with agents that facilitate homing to memory niches, it could be effectively incorporated into vaccination strategies to enhance long-term T cell persistence.

However, ruxolitinib's interaction with Pgp also raises considerations for drug-drug interactions, as ruxolitinib may compete with other Pgp substrates for efflux and alter local drug concentrations within tissues.

3.5. Limitations and Future Directions

This study was conducted primarily using in vitro models, which, while informative, may not fully capture the complexity of immune interactions in vivo. Future studies should validate these findings in animal models or additional clinical samples, assess the long-term effects of ruxolitinib on memory T cell survival and function, and dissect the signaling pathways, JAK1/2 versus ROCK-dependent, that mediate the observed effects on migration and differentiation. Investigating how Pgp modulation differentially affects naive, effector, and memory T cell subsets will also be crucial for optimizing therapeutic strategies.

4. Materials and Methods

Antibodies and chemicals.

The following fluorescently-labeled monoclonal antibodies (mAbs) were applied. Mouse anti-human CD8 Allophycocyanin-Hilite7 (APC-H7) (Becton Dickinson, Hungary). Mouse anti-human CD279 (PD-1) Allophycocyanin-Cyanine7 (APC-Cy7) (BioLegend, Biomedica Hungária Kft., Budapest, Hungary). The anti-human CD8 (OKT8) PO and Pgp (15D3) Alexa Fluor 647 dye-labeled mouse mAbs were produced in-house from hybridoma and mouse ascites.

The anti-human CD8 mouse mAb was isolated from the supernatant of OKT8 hybridoma cells. OKT8 cells were cultured in RPMI medium, and the supernatant was collected and purified using a Protein-A column at 4°C.

Isolation and purification of 15D3 and OKT8 antibodies.

The 15D3 anti-human Pgp mouse mAb was purified from mouse ascites [39]. One million 15D3-hybridoma cells were injected intraperitoneally into female BALB/C and Swiss nude mice aged ten weeks. Mice were housed in the animal facility of the University of Debrecen, Life Science Building, Hungary, where conditions were controlled to maintain a temperature range of 21-25°C and a 12-hour light/dark cycle. The mice had free access to standard mice pellets and water ad libitum within standard mice cages. On the 14th day of post-injection, ascites were collected aseptically from the mice and stored at -80°C. The collected ascites were purified using a protein-G column kit (Thermo Fisher Scientific NAbTM Protein G Spin Kit), following the manufacturer's instructions.

 doi:10.20944/preprints202505.0512.v1

The protein concentration of the isolated 15D3 and OKT8 mAbs was measured using a NanoDropTM OneC microvolume UV-Vis Spectrophotometer at 280 nm. 0.02% sodium azide solution was added to the purified antibodies, which were then stored at 44°Cfor short-term storage or at -20°C for long-term storage. Furthermore, according to manufacturer's instructions, Alexa Fluor and PO-labeled mAbs were prepared for direct immunolabeling purposes (Thermo Fisher Scientific, Budapest, Hungary).

The chemicals not specifically indicated were purchased from Thermo Fisher Scientific, Budapest, Hungary, or Sigma-Aldrich, Merck Life Science Kft., Budapest, Hungary).

Cell lines and generation of cytotoxic T lymphocytes.

The P-glycoprotein (MDR1/ABCB1) expressing cells, designated as NIH-3T3 MDR1, and their parental NIH-3T3 mouse fibroblast cell lines were obtained originally from the laboratory of Michel Gottesman, NIH, USA. The JY cell line is a human Epstein–Barr virus-transformed B-lymphoblastoid cell line that expresses a high density of MHC class I A2 and class II DR on the surface plasma membrane [22,23]. Cell lines were maintained in RPMI 1640 medium (Sigma-Aldrich, Merck Life Science Kft., Budapest, Hungary) supplemented with sodium bicarbonate, glucose, pyruvate, MEM non-essential amino acids, GlutaMAX, gentamycin, or ampicillin, and 10% heat-inactivated FCS (SEBAC, Aidenbach, Germany) (complete medium) in a 5% CO2 at 37°C.

CTLs were generated from human peripheral blood lymphocytes (PBL). First, peripheral blood mononuclear cells (PBMCs) were isolated from leukocyte-enriched buffy coats obtained from healthy donors. PBMCs were separated by a standard density gradient centrifugation using Ficoll-Paque Plus (Amersham Biosciences, Uppsala, Sweden). Then, monocytes were removed from PBMCs by positive selection using immunomagnetic cell separation with anti-CD14-conjugated microbeads (Miltenyi Biotec, FRANK Diagnosztika Kft., Budapest, Hungary), according to the manufacturer's instructions. The resultant PBLs were cultured at a density of 2-5 million cells/mL for a few days in T75 tissue culture flasks in a complete RPMI medium supplemented with 10 mM Hepes buffer (pH 7.3) and 50 μM 2-mercaptoethanol (SERVA, Heidelberg, Germany), until used for experiments or stored frozen for long-term preservation. When required, 20 IU of human recombinant IL-2 (PeproTech) was also added to the complete medium.

CTLs were generated by priming PBLs with heat-treated JY antigen-presenting cells in mixed cultures at a 4:1 ratio following procedures outlined in previous research. The JY cells were heat-shocked at 45°C for 2 hours to block their proliferation. After the third day of cell mixing, 20 IU of IL-2 was added to the culture medium every third day, and the cells were cultured for 30 days. The priming was then repeated for another 30-day cycle. It is known that long-term low-level IL-2 promotes memory T-cell development [40].

Measurement of P-glycoprotein and CD8 protein on cell surfaces.

In this procedure, T cells were initially washed with PBS by centrifugation at 1200 rpm for 5 minutes. After the washing step, the cells were counted using a hemocytometer and adjusted to a concentration of 5 million cells per mL. Subsequently, 250,000 cells were plated in a 96-well format. To facilitate the detection of P-glycoprotein and CD8, we added 10 μg/mL of Alexa647-15D3 anti-Pgp antibody and 10 μg/mL of Alexa488-OKT8 anti-CD8 antibody to the cells. The suspension was gently mixed and allowed to incubate on ice for 45 minutes. After incubation, the cells were washed twice with ice-cold glucose PBS to remove unbound antibodies. The cells were then resuspended in ice-cold glucose PBS containing 2 μM Hoechst dye. Pgp intensity measurements were subsequently performed using a Novocyte 3000 RYB flow cytometer.

Real-time quantitative PCR

Total RNA was isolated with TRIzolate Reagent (UD GenoMed) and reverse transcribed to cDNA using a High-Capacity cDNA Reverse Transcription kit (Applied Biosystems) according to the manufacturer's protocol. The amount of mRNA was determined by real-time q-PCR using TaqMan probes: Hs00184500_m1 ABCB1 [41], Hs00184500_m1 ACTB, Mm02619580_g1 Actb, Hs02786624_g1 GAPDH and Mm99999915_g1 Gapdh. Real-time monitoring was done using a LightCycler 480 Instrument II (Roche). Gene expression normalization was conducted using both human and mouse

 doi:10.20944/preprints202505.0512.v1

β-actin and GAPDH reference genes, selected based on housekeeping gene stability analysis using the RefFinder tool. Gene expression was determined by the delta-delta cycle threshold ($\Delta\Delta C_T$) method.

Transport activity factor assessment via calcein accumulation assay.

The transport activity factor was evaluated using adherent NIH-MDR1 and NIH-3T3 cell lines maintained at 80-90% confluence. The cells were thoroughly washed twice with 1x PBS, followed by trypsinization. The resulting cell suspension was counted using a hemocytometer and resuspended in 10 mL of 8 mM glucose PBS containing 1% FBS. This suspension was centrifuged at 1200 rpm for 5 minutes. After centrifugation, the supernatant was carefully discarded, and the pellet was resuspended in 1x 8 mM glucose-PBS to achieve a cell concentration of $20 \cdot 10^6$ cells/mL. Similarly, suspension cells were washed twice with 1x PBS, reaching a final concentration of $20 \cdot 10^6$ cells/ml using 1x glucose-PBS. The cells were then equally distributed into sorter tubes, with each tube containing $0.5 \cdot 10^6$ cells. P-glycoprotein inhibitors, Zosuquidar (1 μM), Cyclosporine A (10 μM), and Ruxolitinib (400 nM), were introduced to the samples. Calcein-AM, recognized as an ABCB1 substrate, was added at a final concentration of 100 nM. The treated cells were incubated under controlled conditions of 37°C and 5% CO2 for a duration of 30 minutes. Subsequent to the incubation period, Alexa-546-15D3 and Alexa647-OKT8 antibodies were introduced into the samples. After an additional 30 minutes, the cells were washed with 3 mL of ice-cold 8 mM glucose-PBS containing 1% FBS to eliminate any excess calcein. The cells were then suspended in 0.5 mL of 2 μM Hoechst (a nuclear dye) and maintained on ice in the dark until measurements were conducted. Flow cytometric analysis was performed utilizing the BD Biosciences FACS Aria III. The transport activity factor of the P-glycoprotein pump was determined by analyzing the difference in dye accumulation within the cells in the presence versus the absence of the inhibitors.

$$\text{TAF calculation: } TAF = (MFI(inh) - MFI(0)) / MFI(inh) \quad (1)$$

MFI (inh): Mean Fluorescence Intensity with inhibitor, MFI (0): Mean Fluorescence Intensity without inhibitor. The TAF ranges from a maximum value of 1 to a minimum value of 0.0. [2,42].

Assessing ABC transporter activity using calcein-AM retention and flow cytometry.

The functional activity of ABC transporters was assessed through the inhibitory effects of specific inhibitors; to achieve this, a calcein accumulation assay was employed [2,24–26]. The ABCB1 inhibitor Zosuquidar and the JAK1/2 kinase inhibitor ruxolitinib were analyzed. Drugs were serially diluted across 12 wells of a U-bottom 96-well plate, ranging from high to low concentrations. Calcein-AM, an ABC substrate, was added to achieve final concentrations of 5 nM for NIH-MDR cells and 1 nM for CTLs. Cells were evenly distributed in wells, with and without calcein-AM, at a density of $5 \cdot 10^5$ cells per well. Following this, anti-CD8 Alexa647-OKT8 antibodies were added, and the treated cells were incubated at 37°C in a controlled environment with 5% CO2 for 30 minutes. After incubation, the cells were washed twice with 200 μL of ice-cold glucose-PBS containing 1% FBS to remove excess calcein-AM. This was performed at 1200 rpm for 5 minutes. The treated cells were then suspended in 150 μL of 20 μg/mL Hoechst (nuclear dye) and maintained on ice in dark conditions. The intensity of calcein was subsequently measured using the Novocyte 3000 RYB flow cytometer.

IC_{50} values were determined using the pharmacological analysis toolkit in GraphPad Prism 8. Transport activity factor (TAF) values were first normalized to the maximum response, based on the corresponding base-10 logarithm of the molar inhibitor concentrations. The dose-response curves were then fitted using the "log(inhibitor) vs. normalized response" model.

Experimental setup of T cell activation and treatment.

TCR-activation of cells was achieved by coating wells of a 24-well plate with 2 μg/mL antibody of the CD3/CD28 Dynabeads and incubating overnight at 4°C. Then, excess antibody was removed with PBS wash, and one million cells from JY-exposed primed and JY-non-exposed unprimed cells were added separately to individual wells (TCR-activated cells). Ruxolitinib (MedChem Express, Hungary) was added to wells separately containing CD3/CD28 (activated and RUX-treated cells).

 doi:10.20944/preprints202505.0512.v1

RUX was added to the wells that included only the cells (RUX-only treated cells), and untreated/unstimulated cells (control cells) were used. The activations and treatments were done for 72 hours (Table 1).

After the incubation period, the cells were counted, and a sample of 250,000 cells from each treatment condition was labeled with specific antibodies: anti-PD1 (APC-tagged), anti-Pgp (Alexa488-tagged UIC2 mAb combined with the Pgp inhibitor zosuquidar), and anti-$CD8^+$ (Pacific Orange-tagged OKT8 mAb) in a 96-well U-bottom plate. The labeling procedure was conducted on ice for 45 minutes in the dark. Following this, the cells were washed once with PBS, resuspended in glucose PBS containing Hoechst, and subsequently analyzed using flow cytometry.

Table 1. CD3/CD28 activation of human primary peripheral blood lymphocytes over 72 hours.

Activation status	Untreated	Drug treated
No	Human PBLs	Human PBLs + RUX
Yes	Human PBLs + CD3/CD28 beads	Human PBLs + CD3/CD28 beads + RUX

Each well contained two million PBLs, treated with the JAK kinase inhibitor ruxolitinib (RUX) at a concentration of 100 nM. Cells were activated using anti-CD3/anti-CD28 antibody-coated beads at 2 μg/mL, with or without RUX treatment, as outlined in the experimental setup described above.

Preparation of membrane suspension for ATPase activity measurements.

To measure Pgp-specific ATPase activity, we applied raw membrane samples prepared from NIH 3T3 mouse fibroblast cells expressing human Pgp at a high level. Membrane samples were prepared by using the methodology by Sarkadi et al. [29] with minor modifications previously described in [30,31]. Cells were harvested by scraping them into ice-cold PBS and washed twice at 300 × g for 5 min. After this point, the whole procedure was done in the presence of protease inhibitor cocktail (Sigma-Aldrich, Budapest) and 0.5 mM phenylmethylsulphonyl fluoride (PMSF) at 4°C to prevent the degradation of membrane proteins. Cells ($120\text{-}150 \cdot 10^6$) were homogenized in ice-cold TMEP buffer (50 mM Tris-HCl (pH 7.0), 50 mM mannitol, 2 mM EGTA, 2 mM DTT) using a glass-Teflon tissue homogenizer. The homogenised cells were then centrifuged at 465 × g for 10 min at 4°C to sediment intact cells and nuclear debris. Then the supernatant containing cellular membranes was centrifuged at 28000 × g for 1 hour at 4°C. After centrifugation, the membrane pellet was resuspended in 1-2 mL TMEP buffer and stored at -80°C until further use. The protein concentration of the membrane suspension was measured by using the Lowry method [28].

ATPase activity measurements.

The Pgp-specific ATPase activity was determined by measuring the amount of inorganic phosphate liberated as a result of ATP hydrolysis. Other membrane-bound ATPases significantly contributing to cellular ATP consumption were blocked by Na-azide (for F0F1 complex), ouabain (for Na+/K+ ATPase), and EGTA (for Ca+2 ATPases) [29]. Membrane samples (5 μg membrane protein/sample) were pre-incubated with the tested drugs (1-100 μM ruxolitinib, 10 μM zosuquidar or 40 μM verapamil) in 60 μl ATPase assay premix (50 mM MOPS, 65 mM KCl, 6.5 mM NaN3, 2.6 mM DTT, 1.28 mM ouabain, 0.65 mM EGTA, pH = 7.0) in the presence or absence of 100 μM Na3VO4 (vanadate) for 10 min at 37°C. Then, the ATPase reaction was initiated by adding 3.5 mM MgATP to each sample. After 25 min incubation at 37°C, the ATPase reaction was stopped by 40 μl 5% SDS, and then the samples were further incubated with 105 μl colour reagent [27] at room temperature for 30 min. Absorbances of the samples were measured at 700 nm using a BioTek Synergy HT plate reader (BioTek Instruments, Winooski, VT, USA), and the amount of released Pi was calculated by preparing a calibration curve using samples with known Pi concentration. Since vanadate is a specific inhibitor of ATP hydrolysis by ABC transporters, the Pgp-specific ATPase activity is determined by calculating the difference between the vanadate-untreated and vanadate-treated sample pairs [29].

 doi:10.20944/preprints202505.0512.v1

Flow cytometry.

Calcein intensity was systematically measured in NIH-3T3 MDR1, NIH-3T3, and CTLs, alongside the expression levels of P-glycoprotein and CD8 in CTLs. Cellular surface staining of lymphocytes was performed using the mAbs detailed above. Briefly, cells were incubated with mAbs for 15 minutes at room temperature, followed by washing with PBS at 1600 RPM for 5 minutes. Later, cells were suspended in 400 µL of PBS for acquisition. These evaluations utilized the Novocyte 3000 RYB and BD Biosciences FACS Aria III flow cytometer. The resulting data from the FACS and flow cytometry analyses were processed using FCS Express version 6.0 Flow Research Edition.

CTL transmigration assay across HUVEC monolayers.

HUVEC isolation and culture. Human umbilical vein endothelial cells were isolated as previously described by Palatka et al. [43] and stored frozen until use. For experiments, cells were thawed and cultured in M199 medium (Biosera) supplemented with 10% heat-inactivated fetal bovine serum (Thermo Fisher Scientific), 100 U/mL penicillin, 100 µg/mL streptomycin, 2.5 µg/mL amphotericin B (Biosera), 2 mM glutamine (Biosera), and 10% Endothelial Cell Growth Medium-2 (Lonza). Cells were maintained at 37°C with 5% CO_2 (Eppendorf) in gelatin-coated T75 flasks until confluence, then detached with trypsin-EDTA and washed with sterile PBS.

HUVEC monolayer preparation. For transmigration assays, 1.5 × 10^5 HUVECs were seeded onto 24-well transwell inserts (5 µm pore size; CellQART) pre-coated with 0.2% gelatin. Medium was refreshed every three days. Monolayer integrity was confirmed by measuring transendothelial electrical resistance (TEER) and by mosaic imaging of Calcein Green-AM-stained live HUVECs using a laser-scanning cytometer (iCys, CompuCyte) after cyclosporin A treatment. Plateaued resistance by day 5 indicated confluency.

CTL processing and transmigration. Human cytotoxic T lymphocytes were labeled with Calcein Green-AM and Hoechst 33342 (Thermo Fisher Scientific). In some experiments, HUVEC monolayers were counterstained with Calcein Red-AM (Invitrogen). CTLs were pretreated overnight with 100 nM ruxolitinib or with varying concentrations (0.04, 0.4, and 4 µg/mL) in complete medium.

For transmigration, 3·10^5 labeled CTLs in 340 µL RPMI 1640 medium supplemented with 0.5% fatty acid-free BSA (Sigma-Aldrich) were added to the upper chambers. Lower wells contained 360 µL RPMI with 500 ng/mL CCL19 chemokine (Sigma-Aldrich) as a chemoattractant. Cells were allowed to migrate for 4 hours at 37°C.

Cells from the upper and lower compartments, as well as from the underside of the inserts (detached by trypsinization), were collected. Calcein Green and Hoechst-positive viable cells were quantified using an Accela NovoCyte flow cytometer and analyzed with FCS Express v6 (De Novo Software).

All conditions were tested in triplicate, and experiments were independently repeated at least three times.

Statistical analysis.

Kolmogorov–Smirnov and Shapiro–Wilk normality tests were used to test the normality of data distribution. For non-normally distributed, nonparametric variables, the Mann-Whitney test, and normally distributed parametric variables, Student's t-test was used to calculate the significant differences.

One-way ANOVA with Tukey's post hoc test for multiple comparisons was employed for internal comparison with the level of significance set at $p<0.05$. Statistical analysis was performed using GraphPad Prism v9.0 (GraphPad Software, Inc., San Diego, USA).

Ethics approval.

Blood samples were obtained with the written consent of voluntary healthy donors through individual donations at the Regional Blood Center of the Hungarian National Blood Transfusion Service (Debrecen, Hungary). This collection was conducted under the written approval (OVSzK 3572-2/2015/5200) of the Director of the National Blood Transfusion Service and the Regional and Institutional Ethics Committee of the University of Debrecen, Medical and Health Science Center (Hungary).

 doi:10.20944/preprints202505.0512.v1

5. Conclusions

In conclusion, our findings reveal that ruxolitinib exerts multifaceted effects on human cytotoxic T lymphocytes, modulating P-glycoprotein expression and activity, suppressing activation-associated surface markers, and impairing chemokine-driven endothelial transmigration. These effects suggest that ruxolitinib may influence T cell differentiation trajectories, migratory behaviors, and functional adaptation to tissue microenvironments.

Notably, while inhibition of Pgp efflux function and ATPase modulation required concentrations higher than typical therapeutic levels, the impairment of CCL19-driven CTL transmigration was observed at clinically relevant serum concentrations, suggesting distinct concentration thresholds for its effects on efflux activity versus migratory behavior.

Given its ability to impair lymphocyte trafficking at clinically relevant concentrations, ruxolitinib may not only suppress pathogenic immune activation, as in graft-versus-host disease (GVHD), but could also be strategically leveraged to influence memory T cell localization during vaccination or immunotherapeutic interventions.

Understanding how JAK inhibition alters immune cell dynamics at both molecular and functional levels may inform the development of optimized therapeutic strategies in transplantation, autoimmune diseases, and cancer immunotherapy. Future studies will be necessary to further elucidate how ruxolitinib shapes memory T cell fate, persistence, and tissue-specific homing in vivo.

Author Contributions: Z.B. conceptualized the research. K.B., A.L., N.G., A.B.P., N.T., K.G., and Z.B. designed the experiments. K.B., A.L., N.G., A.B.P., and N.T. performed experiments and measurements and collected data. K.B. and Z.B. wrote the draft. Z.B. finalized the paper. Z.B. supervised and administered the project. Z.B. funding acquisition. All authors have read and agreed to the published version of the manuscript.

Funding: Financial support to Z.B. was provided by the University of Debrecen (OTKA Bridging Research Fund; Science Financing Support; Publication Science Support Program; DETKA-2024 Scientific Research Bridging Fund). A Stipendium Hungaricum scholarship supported the work of K.B. and A.L.

Acknowledgments: We extend our sincere thanks to Edina Nagy, Adél Vezendiné Nagy, Rita Katalin Utasi-Szabó, Anikó Szilágyi from the Department of Biophysics and Cell Biology, Dr. Anett Mázló from the Department of Immunology, and Dr. Katalin Kovács from the Institute of Medical Chemistry, all of them from the University of Debrecen, Hungary, whose dedication and contributions were instrumental in the completion of this article. I am also grateful to Dr. James Nyabuga Nyariki, from the Department of Biochemistry and Biotechnology of the Technical University of Kenya, for his insightful suggestions and dedicated support in critically reviewing the manuscript.

Conflicts of Interest: The authors declare no conflicts of interest.

References

1. Gottesman, M. M.; Fojo, T.; Bates, S. E., Multidrug resistance in cancer: role of ATP-dependent transporters. *Nat Rev Cancer* **2002,** 2, (1), 48-58.
2. Sarkadi, B.; Homolya, L.; Szakacs, G.; Varadi, A., Human multidrug resistance ABCB and ABCG transporters: participation in a chemoimmunity defense system. *Physiol Rev* **2006,** 86, (4), 1179-236.
3. Ueda, K.; Cornwell, M. M.; Gottesman, M. M.; Pastan, I.; Roninson, I. B.; Ling, V.; Riordan, J. R., The mdr1 gene, responsible for multidrug-resistance, codes for P-glycoprotein. *Biochem Biophys Res Commun* **1986,** 141, (3), 956-62.
4. Bossennec, M.; Di Roio, A.; Caux, C.; Menetrier-Caux, C., MDR1 in immunity: friend or foe? *Oncoimmunology* **2018,** 7, (12), e1499388.

 doi:10.20944/preprints202505.0512.v1

5. Chen, M. L.; Sun, A.; Cao, W.; Eliason, A.; Mendez, K. M.; Getzler, A. J.; Tsuda, S.; Diao, H.; Mukori, C.; Bruno, N. E.; Kim, S. Y.; Pipkin, M. E.; Koralov, S. B.; Sundrud, M. S., Physiological expression and function of the MDR1 transporter in cytotoxic T lymphocytes. *J Exp Med* **2020,** 217, (5).
6. Pendse, S. S.; Briscoe, D. M.; Frank, M. H., P-glycoprotein and alloimmune T-cell activation. *Clin Appl Immunol Rev* **2003,** 4, (1), 3-14.
7. Thurm, C.; Schraven, B.; Kahlfuss, S., ABC Transporters in T Cell-Mediated Physiological and Pathological Immune Responses. *Int J Mol Sci* **2021,** 22, (17).
8. Boddupalli, C. S.; Nair, S.; Gray, S. M.; Nowyhed, H. N.; Verma, R.; Gibson, J. A.; Abraham, C.; Narayan, D.; Vasquez, J.; Hedrick, C. C.; Flavell, R. A.; Dhodapkar, K. M.; Kaech, S. M.; Dhodapkar, M. V., ABC transporters and NR4A1 identify a quiescent subset of tissue-resident memory T cells. *J Clin Invest* **2016,** 126, (10), 3905-3916.
9. Murata, K.; Tsukahara, T.; Emori, M.; Shibayama, Y.; Mizushima, E.; Matsumiya, H.; Yamashita, K.; Kaya, M.; Hirohashi, Y.; Kanaseki, T.; Kubo, T.; Himi, T.; Ichimiya, S.; Yamashita, T.; Sato, N.; Torigoe, T., Identification of a novel human memory T-cell population with the characteristics of stem-like chemo-resistance. *Oncoimmunology* **2016,** 5, (6), e1165376.
10. Seelig, A., P-Glycoprotein: One Mechanism, Many Tasks and the Consequences for Pharmacotherapy of Cancers. *Front Oncol* **2020,** 10, 576559.
11. Eadie, L. N.; Hughes, T. P.; White, D. L., Interaction of the efflux transporters ABCB1 and ABCG2 with imatinib, nilotinib, and dasatinib. *Clin Pharmacol Ther* **2014,** 95, (3), 294-306.
12. McKinnell, Z.; Karel, D.; Tuerff, D.; Sh Abrahim, M.; Nassereddine, S., Acute Myeloid Leukemia Following Myeloproliferative Neoplasms: A Review of What We Know, What We Do Not Know, and Emerging Treatment Strategies. *J Hematol* **2022,** 11, (6), 197-209.
13. Bader, M. S.; Meyer, S. C., JAK2 in Myeloproliferative Neoplasms: Still a Protagonist. *Pharmaceuticals (Basel)* **2022,** 15, (2).
14. Elli, E. M.; Barate, C.; Mendicino, F.; Palandri, F.; Palumbo, G. A., Mechanisms Underlying the Anti-inflammatory and Immunosuppressive Activity of Ruxolitinib. *Front Oncol* **2019,** 9, 1186.
15. Veletic, I.; Prijic, S.; Manshouri, T.; Nogueras-Gonzalez, G. M.; Verstovsek, S.; Estrov, Z., Altered T-cell subset repertoire affects treatment outcome of patients with myelofibrosis. *Haematologica* **2021,** 106, (9), 2384-2396.
16. Verbeke, D.; Gielen, O.; Jacobs, K.; Boeckx, N.; De Keersmaecker, K.; Maertens, J.; Uyttebroeck, A.; Segers, H.; Cools, J., Ruxolitinib Synergizes With Dexamethasone for the Treatment of T-cell Acute Lymphoblastic Leukemia. *Hemasphere* **2019,** 3, (6), e310.
17. Ebert, C.; Perner, F.; Wolleschak, D.; Schnoder, T. M.; Fischer, T.; Heidel, F. H., Expression and function of ABC-transporter protein ABCB1 correlates with inhibitory capacity of Ruxolitinib in vitro and in vivo. *Haematologica* **2016,** 101, (3), e81-5.
18. Isberner, N.; Kraus, S.; Grigoleit, G. U.; Aghai, F.; Kurlbaum, M.; Zimmermann, S.; Klinker, H.; Scherf-Clavel, O., Ruxolitinib exposure in patients with acute and chronic graft versus host disease in routine clinical practice-a prospective single-center trial. *Cancer Chemother Pharmacol* **2021,** 88, (6), 973-983.
19. Rekik, R.; Belhadj Hmida, N.; Ben Hmid, A.; Zamali, I.; Kammoun, N.; Ben Ahmed, M., PD-1 induction through TCR activation is partially regulated by endogenous TGF-beta. *Cell Mol Immunol* **2015,** 12, (5), 648-9.
20. Ortega, M. A.; Boaru, D. L.; De Leon-Oliva, D.; Fraile-Martinez, O.; Garcia-Montero, C.; Rios, L.; Garrido-Gil, M. J.; Barrena-Blazquez, S.; Minaya-Bravo, A. M.; Rios-Parra, A.; Alvarez-Mon, M.; Jimenez-Alvarez, L.; Lopez-Gonzalez, L.; Guijarro, L. G.; Diaz, R.; Saez, M. A., PD-1/PD-L1 axis: implications in immune regulation, cancer progression, and translational applications. *J Mol Med (Berl)* **2024,** 102, (8), 987-1000.

 doi:10.20944/preprints202505.0512.v1

21. Chen, H.; Li, M.; Ng, N.; Yu, E.; Bujarski, S.; Yin, Z.; Wen, M.; Hekmati, T.; Field, D.; Wang, J.; Nassir, I.; Yu, J.; Huang, J.; Daniely, D.; Wang, C. S.; Xu, N.; Spektor, T. M.; Berenson, J. R., Ruxolitinib reverses checkpoint inhibition by reducing programmed cell death ligand-1 (PD-L1) expression and increases anti-tumour effects of T cells in multiple myeloma. *Br J Haematol* **2021,** 192, (3), 568-576.
22. Bacso, Z.; Bene, L.; Bodnar, A.; Matko, J.; Damjanovich, S., A photobleaching energy transfer analysis of CD8/MHC-I and LFA-1/ICAM-1 interactions in CTL-target cell conjugates. *Immunol Lett* **1996,** 54, (2-3), 151-6.
23. Biwott, K.; Singh, P.; Barath, S.; Nyariki, J. N.; Hevessy, Z.; Bacso, Z., Dynamic P-glycoprotein expression in early and late memory states of human CD8 + T cells and the protective role of ruxolitinib. *Biomed Pharmacother* **2025,** 182, 117780.
24. Hollo, Z.; Homolya, L.; Davis, C. W.; Sarkadi, B., Calcein accumulation as a fluorometric functional assay of the multidrug transporter. *Biochim Biophys Acta* **1994,** 1191, (2), 384-8.
25. Homolya, L.; Hollo, Z.; Germann, U. A.; Pastan, I.; Gottesman, M. M.; Sarkadi, B., Fluorescent cellular indicators are extruded by the multidrug resistance protein. *J Biol Chem* **1993,** 268, (29), 21493-6.
26. Strouse, J. J.; Ivnitski-Steele, I.; Waller, A.; Young, S. M.; Perez, D.; Evangelisti, A. M.; Ursu, O.; Bologa, C. G.; Carter, M. B.; Salas, V. M.; Tegos, G.; Larson, R. S.; Oprea, T. I.; Edwards, B. S.; Sklar, L. A., Fluorescent substrates for flow cytometric evaluation of efflux inhibition in ABCB1, ABCC1, and ABCG2 transporters. *Anal Biochem* **2013,** 437, (1), 77-87.
27. Krasznai, Z. T.; Trencsenyi, G.; Krasznai, Z.; Mikecz, P.; Nizsaloczki, E.; Szaloki, G.; Szabo, J. P.; Balkay, L.; Marian, T.; Goda, K., (1)(8)FDG a PET tumor diagnostic tracer is not a substrate of the ABC transporter P-glycoprotein. *Eur J Pharm Sci* **2014,** 64, 1-8.
28. Lowry, O. H.; Rosebrough, N. J.; Farr, A. L.; Randall, R. J., Protein measurement with the Folin phenol reagent. *J Biol Chem* **1951,** 193, (1), 265-75.
29. Sarkadi, B.; Price, E. M.; Boucher, R. C.; Germann, U. A.; Scarborough, G. A., Expression of the human multidrug resistance cDNA in insect cells generates a high activity drug-stimulated membrane ATPase. *J Biol Chem* **1992,** 267, (7), 4854-8.
30. Tarapcsak, S.; Szaloki, G.; Telbisz, A.; Gyongy, Z.; Matuz, K.; Csosz, E.; Nagy, P.; Holb, I. J.; Ruhl, R.; Nagy, L.; Szabo, G.; Goda, K., Interactions of retinoids with the ABC transporters P-glycoprotein and Breast Cancer Resistance Protein. *Sci Rep* **2017,** 7, 41376.
31. Trencsenyi, G.; Kertesz, I.; Krasznai, Z. T.; Mate, G.; Szaloki, G.; Szabo Judit, P.; Karpati, L.; Krasznai, Z.; Marian, T.; Goda, K., 2'[(18)F]-fluoroethylrhodamine B is a promising radiotracer to measure P-glycoprotein function. *Eur J Pharm Sci* **2015,** 74, 27-35.
32. Chu, T.; Zehn, D., Charting the Roadmap of T Cell Exhaustion. *Immunity* **2020,** 52, (5), 724-726.
33. Zak, J.; Pratumchai, I.; Marro, B. S.; Marquardt, K. L.; Zavareh, R. B.; Lairson, L. L.; Oldstone, M. B. A.; Varner, J. A.; Hegerova, L.; Cao, Q.; Farooq, U.; Kenkre, V. P.; Bachanova, V.; Teijaro, J. R., JAK inhibition enhances checkpoint blockade immunotherapy in patients with Hodgkin lymphoma. *Science* **2024,** 384, (6702), eade8520.
34. Schurch, C. M.; Caraccio, C.; Nolte, M. A., Diversity, localization, and (patho)physiology of mature lymphocyte populations in the bone marrow. *Blood* **2021,** 137, (22), 3015-3026.
35. Rudolph, J.; Heine, A.; Quast, T.; Kolanus, W.; Trebicka, J.; Brossart, P.; Wolf, D., The JAK inhibitor ruxolitinib impairs dendritic cell migration via off-target inhibition of ROCK. *Leukemia* **2016,** 30, (10), 2119-2123.
36. Stein, J. V.; Soriano, S. F.; M'Rini, C.; Nombela-Arrieta, C.; de Buitrago, G. G.; Rodriguez-Frade, J. M.; Mellado, M.; Girard, J. P.; Martinez, A. C., CCR7-mediated physiological lymphocyte homing involves activation of a tyrosine kinase pathway. *Blood* **2003,** 101, (1), 38-44.

 doi:10.20944/preprints202505.0512.v1

37. Heine, A.; Held, S. A.; Daecke, S. N.; Wallner, S.; Yajnanarayana, S. P.; Kurts, C.; Wolf, D.; Brossart, P., The JAK-inhibitor ruxolitinib impairs dendritic cell function in vitro and in vivo. *Blood* **2013,** 122, (7), 1192-202.
38. McCoy, S. S.; Parker, M.; Gurevic, I.; Das, R.; Pennati, A.; Galipeau, J., Ruxolitinib inhibits IFNgamma-stimulated Sjogren's salivary gland MSC HLA-DR expression and chemokine-dependent T cell migration. *Rheumatology (Oxford)* **2022,** 61, (10), 4207-4218.
39. Gellen, G.; Klement, E.; Biwott, K.; Schlosser, G.; Kallo, G.; Csosz, E.; Medzihradszky, K. F.; Bacso, Z., Cross-Linking Mass Spectrometry on P-Glycoprotein. *Int J Mol Sci* **2023,** 24, (13).
40. Kalia, V.; Sarkar, S., Regulation of Effector and Memory CD8 T Cell Differentiation by IL-2-A Balancing Act. *Front Immunol* **2018,** 9, 2987.
41. Sorf, A.; Sucha, S.; Morell, A.; Novotna, E.; Staud, F.; Zavrelova, A.; Visek, B.; Wsol, V.; Ceckova, M., Targeting Pharmacokinetic Drug Resistance in Acute Myeloid Leukemia Cells with CDK4/6 Inhibitors. *Cancers (Basel)* **2020,** 12, (6).
42. Goda, K.; Donmez-Cakil, Y.; Tarapcsak, S.; Szaloki, G.; Szollosi, D.; Parveen, Z.; Turk, D.; Szakacs, G.; Chiba, P.; Stockner, T., Human ABCB1 with an ABCB11-like degenerate nucleotide binding site maintains transport activity by avoiding nucleotide occlusion. *PLoS Genet* **2020,** 16, (10), e1009016.
43. Palatka, K.; Serfozo, Z.; Vereb, Z.; Batori, R.; Lontay, B.; Hargitay, Z.; Nemes, Z.; Udvardy, M.; Erdodi, F.; Altorjay, I., Effect of IBD sera on expression of inducible and endothelial nitric oxide synthase in human umbilical vein endothelial cells. *World J Gastroenterol* **2006,** 12, (11), 1730-8.